

Theoretical study of short electrostatic lens for the Columbia ion microprobe

Alexander D. Dymnikov,^{a)} David J. Brenner, Gary Johnson,
and Gerhard Randers-Pehrson
RARAF, Columbia University, 136 South Broadway, Irvington, New York 10533

(Received 4 November 1999; accepted for publication 13 December 1999)

A short probe-forming system is developed for the Columbia Microprobe that includes four electrostatic quadrupoles with a Russian quadruplet configuration. The smallest beam spot size and appropriate optimal parameters of the probe-forming systems have been found. These parameters of the system are compared with appropriate parameters of other field configurations including the electrostatic and magnetic fields with dipole, quadrupole, and rotational symmetry. The new original construction of the electrostatic quadruplet has been manufactured. The sensitivity of this quadruplet to some misalignments of the construction is investigated. © 2000 American Institute of Physics. [S0034-6748(00)01404-0]

I. INTRODUCTION

Microscopy with high-energy ions is a relatively novel technique. The first nuclear microprobe¹ with the magnetic Russian quadruplet lens focusing² built in 1970 opened up many new investigative fields. Now an expanding number of laboratories are applying nuclear microprobes to a very wide range of problems in science and technology. Microbeams are used in biology and medicine, in microelectronics and photonics, in arts and archaeology, in geology and planetary science, in environmental science, in ion lithography, and in material science.³

Focusing of ion beams of MeV energy is usually accomplished by quadrupole lenses. The great majority of these employ a combination of magnetic quadrupole lenses.^{4,5} Another way to obtain a microbeam is to use solenoids as probe-forming lenses. But manufactured coils do not have a perfect rotational symmetry. Existing microprobes with solenoids do not produce the resolution of less than a few microns.⁶

At the Center for Radiological Research of Columbia University we are planning two ion microprobes to study the response of biological cells to irradiation with single ions. This article is devoted to the first (preliminary) design having the following geometry. The total length $l_t = 1.3$ m (the distance between the object slit and the target), the lens length $l = 0.26$ m (the sum of all lengths of lenses and spaces between lenses), and the working distance $g = 0.1$ m (the distance between the last lens and the target). The demagnifications in the xoz and $yo z$ planes are d_1 and d_2 , respectively. The purpose of this design with rather small negative demagnification ($d_1 = d_2 = -4.2$) is to be a prototype for the final design with $l_t = 3.7$ m and with rather big positive demagnification ($d_1 = d_2 \sim 50-80$).

The preliminary microprobe lens design is chosen as is the electrostatic Russian quadruplet (RQE). Analytical and numerical matrix methods are developed to obtain the mini-

mum spot size and appropriate optimal parameters of RQE and the other probe-forming systems. The optimal parameters for the first design are found and they are compared with corresponding results for other lenses with different field configurations but with the same geometry and demagnification. These configurations include electrostatic (TQE) and magnetic (TQM) triplets, magnetic Russian quadruplet (RQM), magnetic solenoids (SolM), coaxial electrostatic cylinders (CylE), and bending magnets (BendM). Some tolerances for the preliminary design are determined and the manufactured original construction of the RQE is described.

II. OPTIMIZATION

We have performed the special program of optimizing analytical and numerical calculations to obtain the best design for our system. Beam focusing is understood as the result of nonlinear motion of a set of particles. As a result of this motion, we have the beam spot on the target. The set has a volume (the phase volume, or emittance). For a given brightness, the phase volume is proportional to the beam current and *vice versa*. The beam has an envelope surface. All particles of the beam are located inside of this surface, inside of this beam envelope. For the same phase volume (or beam current) the shape of the beam envelope can be different. We say the beam envelope is *optimal* if the spot size on the target has a *minimum* value for a given emittance. The beam of a given emittance is defined by a set of two matching slits: objective and divergence slits. For a given emittance em , the shape of the beam envelope is the function of the half-width (or radius) r_1 of the objective slit and of the distance l_{12} between two slits. The size r_2 of the second (divergence) slit is determined by the expression: $r_2 = em \times l_{12}/r_1$. The optimal parameters r_1 , r_2 , and l_{12} determine the *optimal beam envelope* or the *optimal matching slits*.

The probe-forming system consists of two systems: the matching slit system and the focusing system. Usually the focusing system has two field parameters (two excitations) and several parameters of its geometry. For this case from

^{a)}Electronic mail: ad455@columbia.edu

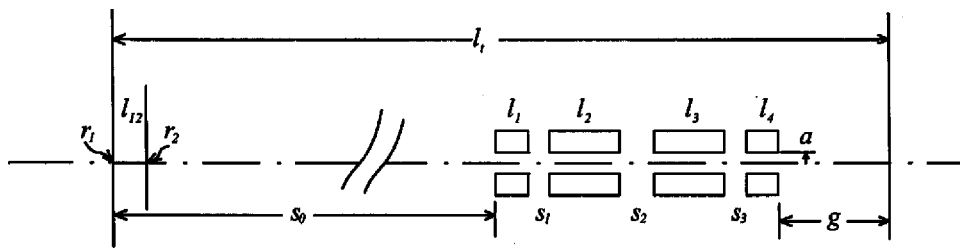


FIG. 1. Geometry of the ion microprobe lens.

two conditions of stigmatism we find the first approximation of two excitations as a function of the geometry. For each geometry we can find the optimal matching slits. The geometry, which gives the smallest spot size, is the *optimal geometry*. For this geometry and for the optimal matching slits we find the *optimal excitations* giving the minimum spot size. The *optimal probe-forming system* comprises the optimal excitations, optimal matching slits, and optimal geometry. For each emittance we find the parameters of the optimal probe-forming system. We consider the nonlinear motion of the beam accurate to terms of third order for systems with rotational or quadrupole symmetry and to terms of second order for systems with dipole symmetry.

To perform an optimal synthesis we use two different figures of merit. The first one is the average radius of the beam. For a given geometry of the focusing system we compute the first approximation of lens excitations, κ_i , which provide the stigmatic property of the system. Then we find the optimal r_1 and l_{12} that give the smallest value of the average radius in the Gaussian image plane for each emittance. But the minimum spot is located at the plane of the circle of least confusion, not at the Gaussian plane. We can move this spot to the Gaussian plane (or to the target plane) by changing the excitations. In the set of n particles we select one particle: the reference (or axial) particle with the coordinates x_r and y_r on the target. At the end of the optimization we take the second figure of merit, ρ , as the maximum value of the $|x - x_r|_{\max}$ and $|y - y_r|_{\max}$ of the particles on the target. After that we determine the optimal lens excitations (the second approximation) that give the minimum ρ , using 1000 particles with randomized position and divergence. This gives us the possibility to obtain the minimum spot without tail.

III. MATRIX APPROACH

The essential feature of our optimization is the matrix approach for nonlinear beam motion. In this approach we obtain and use analytical expressions for the matrizant (or transfer matrix) and for the envelope matrix. This matrix technique is known as the Matrizant method.⁷ We use this technique for solving the equations of motion, the nonlinear differential equations in four-dimensional phase space, for example, for the field with the rotational or quadrupole symmetry accurate to terms of the third order. These equations are replaced by two vector linear equations (for x and y planes) in the 12-dimensional phase moment space or by one equation in the 24-dimensional phase moment space. Writing the nonlinear equations in a linearized form allows us to construct the solution using a 12×12 (or 24×24) third order

matrizant. For the field with the dipole symmetry we use the nonlinear differential equations in four-dimensional phase space accurate to terms of the second order. For this case we obtain a 14×14 matrizant of the second order.

As a result of this linearization it becomes possible to use all the advantages of linear differential equations over nonlinear ones, including the independence of the matrizant of the choice of the initial point of the phase space.

Assuming a uniform density of particles in the plane of the two slits, knowing the third order matrizant and choosing by a random method N particles we can obtain the position of these particles in the image plane or in the target (or specimen) plane.

From the matrizant we can also find the spherical aberration coefficients in the object space csx , csy , and $csxy$. For the fields with rotational or quadrupole symmetry (with the third order matrizant) these coefficients⁸ in the image space are written in the form: $csx_{im} = csx/d_1^3$, $csy_{im} = csy/d_2^3$, $csxy_{im} = csxy/d_1d_2^2 = csyx/d_2d_1^2$. For the fields with dipole symmetry (with the second order matrizant) these coefficients in the image space are written in the following form: $csx_{im} = csx/d_1^2$, $csy_{im} = csy/d_2^2$, $csxy_{im} = csxy/d_1d_2 = csyx/d_2d_1$. We define C_{im} as the maximum value of $|csx_{im}|$ and $|csy_{im}|$.

We study the evolution of the phase moment vector, which contains the elements of the phase moments of first and third order. The envelope matrix is taken as the matrix of the second moments of the distribution of this vector over the totality of the phase coordinates. We consider the case of a small density beam; then, beam self-field as well as particle collisions can be neglected and the distribution function satisfies the Liouville's equation. The integration is done over the object and aperture slits. We find the analytical form of the 12×12 (or 24×24) initial envelope matrix for the fields with rotational or quadrupole symmetry or (a 14×14 matrix for the fields with the dipole symmetry) as a function of em , r_1 , and l_{12} . This matrix is normalized by equating the first diagonal element to r_1^2 . Thus the average radius of the beam is determined by the first diagonal element of the envelope matrix, which is a function of the position along the axis.

IV. THE OPTIMAL PROTOTYPE LENS SYSTEM

We have chosen an electrostatic focusing system because its focusing strength depends only on the accelerating voltage used to produce the ions. This is important for us because we intend to add heavy ion capability to our system.

Our RQE, the geometry of which is shown in Fig. 1, consists of four quadrupoles, each of them formed by four cylindrical rods with the same radius r and semiaperture a

and with length l_i . Geometrical and electrical data are the following ones: the distance s_0 of the first quadrupole to the object aperture, the separation s_i between the i th and $i+1$ th quadrupoles; finally the polarization is chosen so that in every plane $V_1 = -V_4$ and $V_2 = -V_3$.

In order to obtain the maximum operating voltage, we want to operate all the lenses at approximately the same voltage ($V_1 \approx -V_2$). That is, they will all be operated near the breakdown strength of the system without having one element be the weak link. We therefore choose the lengths of the electrodes such that the proper focusing will be obtained with essentially the same voltage on each electrode.

As a result of our optimization we have obtained the following optimal parameters: $r = a = 5$ mm, $l_1 = l_4 = 3$ cm, $l_2 = l_3 = 6.5$ cm, $s_0 = 94$ cm, $s_1 = s_3 = 2$ cm, $s_2 = 3$ cm, $V_1 \approx -V_2 \approx 15$ kV (for 3 MeV protons).

We have found the following values of the minimum spot size ρ , optimal r_1 , r_2 in μm and l_{12} in mm for three emittances. For $em = 1 \mu\text{m} \times \text{mrad}$: $\rho = 0.508$, $r_1 = 1.859$, $r_2 = 5.133$, $l_{12} = 9.54$. For $em = 3 \mu\text{m} \times \text{mrad}$: $\rho = 1.18$, $r_1 = 4.47$, $r_2 = 10.215$, $l_{12} = 15.1$. For $em = 10 \mu\text{m} \times \text{mrad}$: $\rho = 2.88$, $r_1 = 10.40$, $r_2 = 24.83$, $l_{12} = 27.4$.

V. COMPARISON OF THE MINIMUM SPOT SIZE AND THE OPTIMAL SLIT PARAMETERS FOR DIFFERENT FIELDS

The best performance of a microprobe focusing lens can be described by the relation of the minimum beam spot size to the emittance. We have compared this minimum and the optimal slit parameters of our prototype system with the appropriate values of other systems. For this purpose we have performed the optimization for six other focusing lenses with

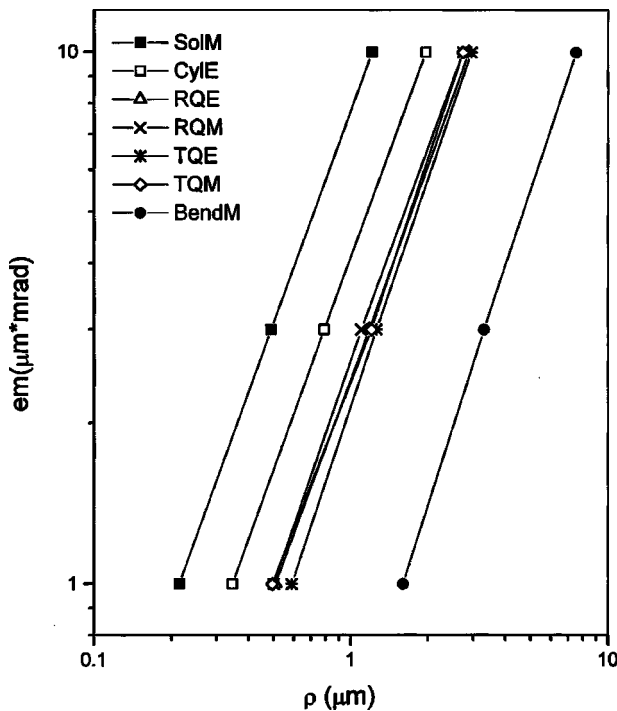


FIG. 2. Plots of the two-dimensional emittance em as functions of the minimum spot size ρ for different microprobe focusing lenses.

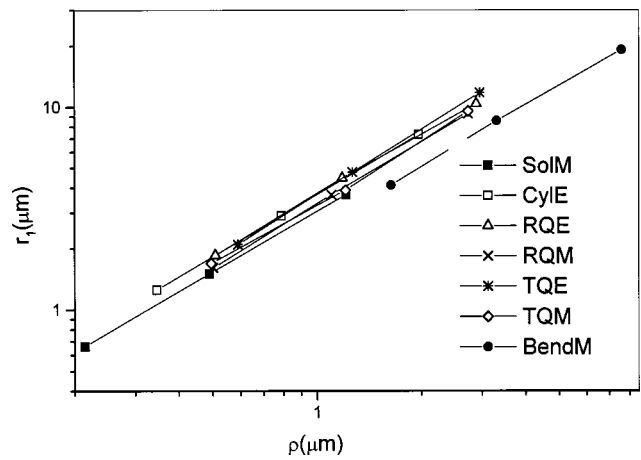


FIG. 3. Plots of the optimal object slit radius r_1 for different microprobe focusing lenses as functions of the minimum spot size ρ .

the same geometry and with the same demagnification as our preliminary design has but with different fields.

For the spherical aberration coefficients C_{im} in the image plane we have obtained the following values in rad^{-3}m : SolM-0.30, CyIE-3.95, RQE-36.12, RQM-10.55, TQE-50.86, TQM-14.95, BendM-1.03.

For the last lens, the bending magnet, we used the non-linear differential equations of the second order and at this case it is not correct to compare the value of the spherical aberration coefficient for the bending magnet with the same coefficients for other lenses.

As the result of our optimization we have obtained the minimum beam spot size and appropriate optimal parameters of the systems for all considered field configurations and for three different emittances for the first mode of excitations with negative, equal in the both planes, demagnification $d = d_1 = d_2 = -4.2$. We can consider these data as the maximum emittance and appropriate optimal parameters of the systems for three different ρ .

In Figs. 2-5 the two-dimensional emittance em and appropriate optimal r_1 , r_2 , and l_{12} for different field configurations are plotted as functions of the minimum beam spot

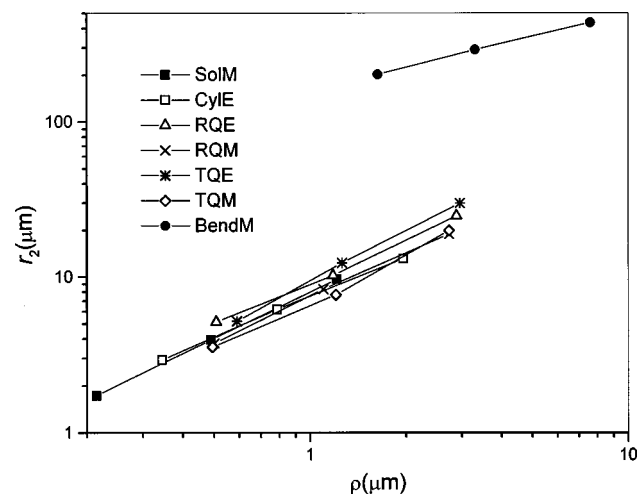


FIG. 4. Plots of the optimal divergence slit radius r_2 for different microprobe focusing lenses as functions of the minimum spot size ρ .

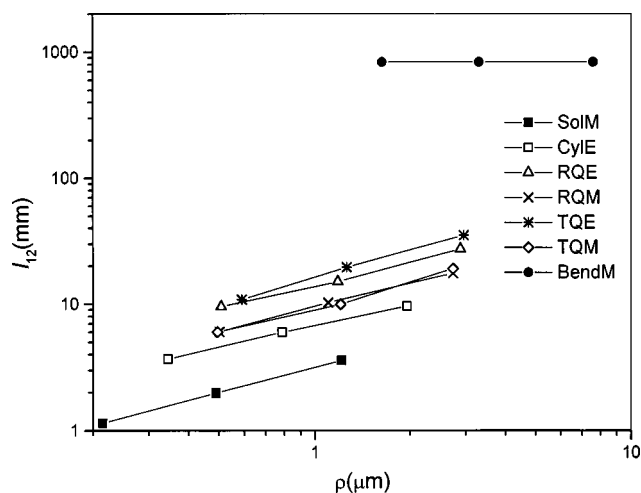


FIG. 5. Plots of the optimal distance between the object and divergence slits for different microprobe focusing lenses as functions of the minimum spot size ρ .

size ρ . We see that in an ideal (without any misalignments and energy spread) magnetic solenoid it is possible to obtain the smallest spot size for a given emittance or the biggest emittance for a given spot size. But it is a mass dependent lens and in a real solenoid this minimum is not achieved at the present time.

The second smallest spot size (or the biggest emittance) is realized in an ideal electrostatic axial symmetrical field but this field has too high of a potential (2.6 MV).

The third smallest spot size for a given emittance is obtained in ideal quadrupole systems. This size is approximately the same for triplets and quadruplets. For the electrostatic quadrupole systems the smallest spot size is achieved in the Russian quadruplet RQE.

It is interesting to note one thing. For the linear (Gaussian) approximation of the equations of the beam particle motion we have only one function (one Gaussian curve) for all fields $r_1 = |d|\rho$. In our case the demagnification $d = -4.2$. But for the nonlinear equations we observe the splitting of this function for seven different curves. All these curves are located above Gaussian curve. This means that in the nonlinear case more demagnification is needed to obtain the same spot size as in the paraxial case.

VI. ABERRATIONS, MISALIGNMENTS AND FABRICATION

A. Influence of the energy spread

We have investigated the influence of the energy spread $\Delta E/E$ (the energy resolution of the accelerator) on the optimal spot for the RQE. To keep the increase in the average radius of the optimal spot less than 10% we need to have $\Delta E/E$ less than 0.0001 for $em = 1 \mu\text{m} \times \text{mrad}$, 0.0002 for $em = 3 \mu\text{m} \times \text{mrad}$, and 0.0004 for $em = 10 \mu\text{m} \times \text{mrad}$. The same results are obtained for the requirements on the stability of the power supply.

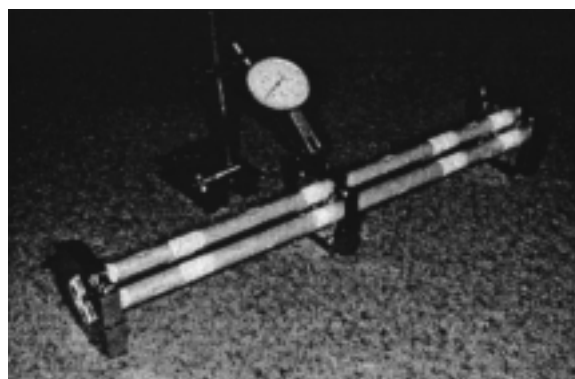


FIG. 6. The photograph of the prototype lens design.

B. Aberration due to misalignment

Increase of the beam spot size can also be caused by a lateral displacement of the slit system with respect to the RQE longitudinal axis. Our calculations show that to limit the increase in the average radius of the optimal spot to less than 10%, we need to have the tolerance for this displacement less than 0.1 mm.

C. Rotational misalignment of the chosen construction

For the chosen construction we can consider the possible small rotation of the entire set of quadrupoles. The performed calculations show that for the increase in the average radius of the optimal spot to be less than 10% we need to have the tolerance for this axial rotation less than 1.2 mrad over the whole length of the lens.

D. Fabrication

One of the main features of the RQE design being used is that part of the alignment of the electrodes is accomplished by using four 0.01 m diameter ceramic (macor) rods 0.3 m long for the entire set of four quadrupoles. The rods will be centerless ground to a tolerance of $6 \mu\text{m}$ for the diameter and $12 \mu\text{m}$ for camber (straightness). This design should essentially eliminate misalignment of the quadrupole axes, which would induce parasitic aberrations. Evaporating a thin layer of gold onto the entire cylindrical surface in bands will create the 16 positive and negative electrodes. The insulating sections between bands will be the original ceramic surface with a relief machined at the end of each section. The photograph of this design is shown in Fig. 6.

After testing the prototype system we will design the optimal final system.

ACKNOWLEDGMENT

This work was supported by Grant No. P41 RR-11623 from the NIH National Center for Research Resources.

¹A. D. Dymnikov and S. Y. Yavor, *Sov. Phys. Tech. Phys.* **8**, 639 (1964).

²J. A. Cookson, R. T. G. Ferguson, and F. D. Pilling, *J. Radioanal. Chem.* **12**, 39 (1972).

³B. L. Doyle, C. J. Maggiore, and G. Bench, *Nuclear Microprobe Technology and Applications* (North-Holland, Amsterdam, 1997).

⁴G. J. F. Legge, Nucl. Instrum. Methods Phys. Res. B **130**, 9 (1997).

⁵P. H. A. Mutsaers, Nucl. Instrum. Methods Phys. Res. B **113**, 323 (1996).

⁶A. Stephan, J. Meijer, M. Hofert, H. H. Bukow, and C. Rolf, Nucl.

Instrum. Methods Phys. Res. B **89**, 420 (1994).

⁷A. D. Dymnikov and R. Hellborg, Nucl. Instrum. Methods Phys. Res. A **330**, 323 (1993).

⁸A. D. Dymnikov, D. N. Jamieson, and G. J. F. Legge, Nucl. Instrum. Methods Phys. Res. B **104**, 64 (1995).